Sigma Journal of Engineering and Natural Sciences
Web page info: https://sigma.yildiz.edu.tr
DOI: 10.14744/sigma.2021.00045

Research Article

Design and analysis of an improved single-phase QUASI-Z-source inverter

Mustafa Sacid ENDİZ[1,*], Ramazan AKKAYA[2]

[1]*Department of Electrical and Electronics Engineering, Necmettin Erbakan University, Konya, 42370,Türkiye*
[2]*Department of Electrical and Electronics Engineering, Konya Technical University, Konya, 42250, Türkiye*

ARTICLE INFO

Article history
Received: 06 May 2021
Revised: 14 July 2021
Accepted: 27 August 2021

Keywords:
Switched-Inductor; Quasi-Z-Source Inverter; Boost Factor

ABSTRACT

In recent years, the traditional power inverter systems have been replaced by the modern impedance source inverter (ZSI) circuit topology which became highly popular due to many benefits such as voltage boosting ability, reduced cost, flexibility, and, less sensitivity to electromagnetic noises. This paper presents an improved single-phase quasi-Z-source inverter (qZSI) circuit model. The input inductor of the qZSI circuit has been replaced by a switched-inductor (SL) configuration which is integrated into DC power source and impedance network. The proposed circuit can make use of the stored DC power with the help of the SL form within the shoot-through time interval. In comparison with the conventional qZSI topology, the proposed model increases the boost factor of the qZSI circuit significantly for the same shoot-through time. In addition to that, the circuit draws continuous input current and shares common ground with DC power source. The operation principle is analyzed with the help of the mathematical equations and simulations are carried out using Matlab/Simulink environment. A laboratory prototype is realized to validate the proposed circuit. Simulation and experimental results are presented to illustrate the performance of the proposed inverter topology. The presented circuit model is open to new developments and can be used for low power applications such as photovoltaic (PV) and fuel cell systems.

Cite this article as: Endiz MS, Akkayam R. Design and analysis of an improved single-phase QUASI-Z-source inverter. Sigma J Eng Nat Sci 2023;41(3):602–612.

INTRODUCTION

Over the last two decades, the impedance source inverter (ZSI) circuit model defined by Peng in 2003 [1] is among the most popular power electronics converter topologies and employed in many industrial applications such as AC motor drives, renewable energy systems, electric vehicles and fuel cell technologies [2]. The basic impedance network of ZSI circuit consists of equal inductors and capacitors connecting power switches with DC power source. During the process of the shoot-through time, the energy generated by DC power source is stored in the inductors. In the period of the non-shoot-through time, the stored energy in the inductors is transferred into the inverter bridge which is called boosting process of the ZSI circuit. Based on the

***Corresponding author.**
*E-mail address: msendiz@erbakan.edu.tr
This paper was recommended for publication in revised form by Regional Editor N. Özlem Ünverdi

operation principle of the ZSI, the power switches of the same leg can be gated on at the same time. Therefore the output voltage can be any desired value depending on the boost factor without giving any damage to DC power source or inverter power switches. Because of the possibility of the shoot-through states in the ZSI, the circuit immunity to electromagnetic interference is higher than in voltage source inverter (VSI) and current source inverter (CSI) [3]. Even though the ZSI has become an advanced topology, it has some drawbacks such as large voltage stress across the components, huge inrush current, and small boost factor. Therefore a new topology called quasi-Z-Source inverter (qZSI) was introduced as shown in Figure 1 [4]. With a modification in the impedance network, the qZSI topology keeps all the advantages of the ZSI topology and eliminates the essential limitations such as non-continuous input current and high capacitor stress. Through the input inductor placed in the impedance network, the qZSI is capable of drawing a continuous constant input current from DC power source and has a lower rated capacitor voltage in C_2. Since the input voltage in photovoltaic (PV) systems varies with the solar radiation and outside temperature, the qZSI topology is more suitable for PV-based applications to obtain a stable and constant output power [4, 5].

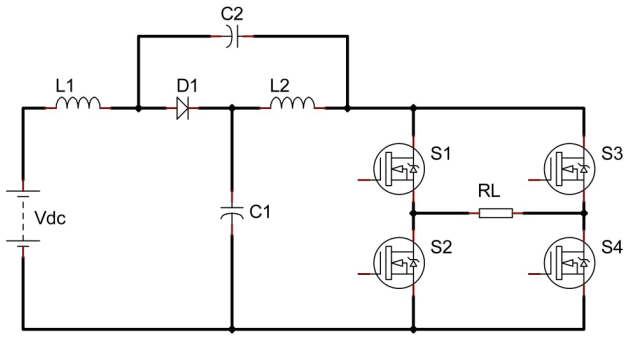

Figure 1. The qZSI circuit topology.

In [6], different PWM-based modulation techniques are reviewed and compared for different voltage types of ZSI/qZSI circuits. For the elimination of the ZSI/qZSI limitations, various circuit topologies are explored and their application backgrounds are widely studied [7-8]. In recent years, switched-inductor (SL) integrated ZSI/qZSI circuit configurations have been presented aiming at the benefits of the voltage boost increasing, reduction of the voltage stresses on capacitors, and current stresses on inductors, continuous input current, and circuit reliability. Minimizing the component rating and producing high DC-link voltage have been the main objectives for the proposed topologies [9, 10]. Dual-input qZSI circuit has been designed and implemented for harvesting more input DC power with higher conversion efficiency [11]. Another proposed qZSI topology has been presented with two-switched impedance networks to increase the boost potential [12]. In [13], the SL configuration has been combined with the switched-capacitors (SC) configuration to enhance the boost factor for renewable energy applications. L-Z-source inverter having only inductors and diodes in Z-source network with the eliminating of the inrush current at startup and two symmetric extended-boost embedded SL qZSI circuit model for getting higher voltage gain with smaller duty cycle ratio have been presented [14, 15]. In [16], a modified SL qZSI is proposed with continuous input current and high boosting capability to obtain an efficient power conversion using three capacitors, three diodes, two inductors, and one switch. Two new ZSI topologies for inverter applications have been designed to increase the boost factor and the elimination of the inrush current at startup by using an additional switch [17]. In [18] is provided the analytical comparison of different SL ZSI and SL qZSI configurations. General classification with its main characteristics can be used for selecting different applications.

Compared with the ZSI/qZSI circuit topologies, this paper presents a qZSI circuit with a modified network. The proposed circuit improves the boost factor and the output voltage using the SL form instead of the input inductor which is integrated into DC power source and impedance network. Unlike the traditional ZSI topology, the proposed circuit draws continuous input current and shares common ground with DC power source. Compared to the traditional qZSI topology, the performance of the voltage conversion ability has increased significantly.

Theory

As shown in Figure 2, the SL circuit form has two equivalent inductors (L_1 and L_3) and three fast recovery diodes (D_2, D_3, and D_4) inside the switched-inductor cell. This configuration composed of passive circuit elements replaces the input inductor of the qZSI and combines V_{DC} and impedance network.

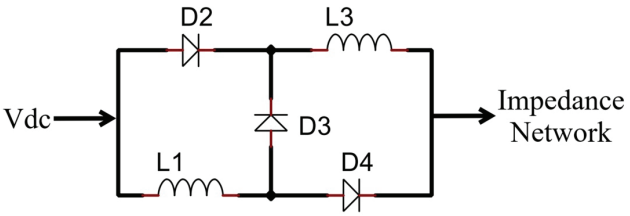

Figure 2. SL circuit form.

The proposed single-phase qZSI with SL circuit form is depicted in Figure 3. As mentioned before, the main issues of the ZSI/qZSI circuits are the limited boost ratio and conversion ability. To overcome these issues, the SL circuit takes the advantage of its operating principles within the

qZSI network. The main idea behind the boost operation principle of the proposed qZSI is based on the employing of the stored energy during the short-circuit process.

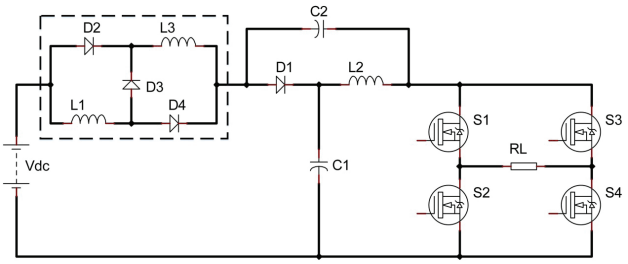

Figure 3. The proposed SL coupled qZSI.

As in the ZSI/qZSI circuits, the proposed qZSI has two operation modes: shoot-through state and non-shoot-through state. To understand the operation principle of the proposed qZSI, two operating states with equivalent circuits are analyzed where V_{DC} is the DC power source, T is the switching cycle, T_0 is the shoot-through cycle, T_1 is the non-shoot-through cycle, M is the modulation index, D is the shoot-through duty ratio, B is the boost factor and V_{PN} is the DC-link voltage across the inverter bridge.

As given in Figure 4, during the shoot-through time interval the qZSI with SL circuit configuration is isolated from the inverter bridge. In this small time interval, DC energy is stored in the SL configuration. The inductors (L_1 and L_3) are connected in parallel with the DC power source and D_1 and D_3 are reverse-biased, while D_2 and D_4 are forward-biased. During the shoot-through process, the energy generated by the DC power source is stored in the inductors (L_1, L_2, and L_3) while the qZSI network is disconnected from the inverter circuit.

The corresponding voltage values of the inductors in the qZSI network for the shoot-through time interval are as follows:

$$V_{L1} = V_{L3} = V_{DC} + V_{C2}, \qquad V_{L2} = V_{C1} \tag{1}$$

As the inductors and capacitors of the qZSI at the shoot-through time interval are connected as shown in the equivalent circuit in Figure4 and D_1 is reversed-biased, the voltages across the qZSI network are:

$$V_{PN} = 0, \qquad V_{D1} = V_{C1} + V_{C2} \tag{2}$$

In the non-shoot-through time interval, the proposed qZSI with SL circuit configuration is illustrated in Figure 5. In this state, the inductors (L_1 and L_3) are connected in series with the DC power source, D_2 and D_4 are reverse-biased, and D_1 are D_3 forward-biased. The energy generated by the DC power source and stored in the inductors (L_1, L_2, and L_3) from the former state is transferred into the inverter bridge. Compared to the amount of the DC power source,

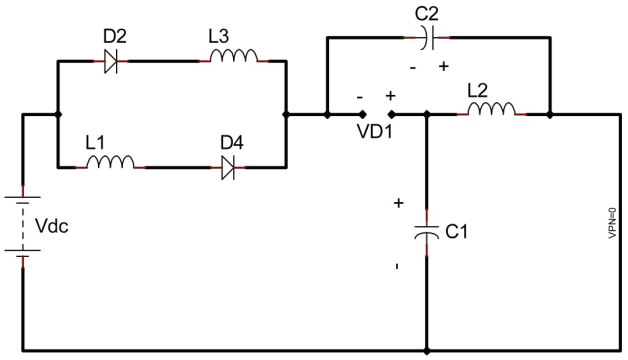

Figure 4. The proposed SL coupled qZSI at the shoot-through time interval.

the transferred DC energy to the AC side is increased since the inductors are connected in series with the DC power source. For the non-shoot-through time corresponding voltage values of the inductors are:

$$V_{L1} = V_{L3} = \frac{(V_{DC} - V_{C1})}{2}, \qquad V_{L2} = -V_{C2} \tag{3}$$

The inductors and capacitors of the qZSI at the non-shoot-through time interval are connected as shown in the equivalent circuit in Figure5 and D_1 is forward-biased, the voltages across the qZSI network are as follows:

$$V_{PN} = V_{C1} + V_{C2}, \qquad V_{D1} = 0 \tag{4}$$

As can be seen in Figure 4 and Figure 5 obviously, the operation process of the proposed qZSI with SL circuit configuration changes according to shoot-through-state and non-shoot-through-state.

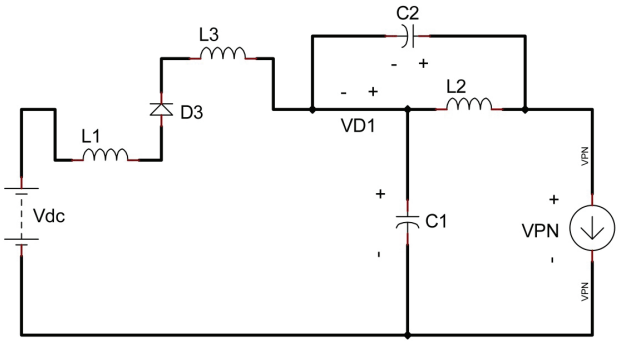

Figure 5. The proposed SL coupled qZSI circuit at the non-shoot-through time interval.

As it is well known at a steady-state, the mean voltage of the inductors (L_1, L_2, and L_3) for a switching cycle T should be zero. Using Eqs. (1) and (3) we get:

$$V_{L1} = V_{L3} = \frac{T_0(V_{DC} + V_{C2})}{T} + \frac{T_1(V_{DC} - V_{C1})/2}{T} = 0 \quad (5)$$

$$V_{L2} = \frac{T_0(V_{C1})}{T} + \frac{T_1(-V_{C2})}{T} = 0 \quad (6)$$

Assuming that $T_0/T = D$ and $T_1/T = 1$ - D, from Eqs. (5) and (6), the capacitor voltages V_{C1} and V_{C2} of the qZSI network, DC-link voltage V_{PN} across the inverter bridge, and the boost factor B are:

$$V_{C1} = \frac{-D^2+1}{-D^2-2D+1}V_{DC}, \quad V_{C2} = \frac{D^2+D}{-D^2-2D+1}V_{DC} \quad (7)$$

$$V_{PN} = V_{C1} + V_{C2} = \frac{D+1}{-D^2-2D+1}V_{DC} = BV_{DC} \Rightarrow B = \frac{D+1}{-D^2-2D+1} \quad (8)$$

For a single-phase inverter operating with sinusoidal PWM; $V_{ac} = MV_{DC}$ where V_{ac} is the peak value of the fundamental of the output voltage, M is the modulation index [1]. Thus, the output peak phase voltage V_{ac} of the proposed qZSI with SL circuit configuration is calculated in Eq. (9):

$$V_{ac} = MV_{PN} = MBV_{DC} = M\frac{D+1}{-D^2-2D+1}V_{DC} \quad (9)$$

Eq. (9) is derived from the product of the modulation index M and Eq. (8). As demonstrated in Eq. (8) obviously, the boost factor B of the qZSI is improved remarkably from $B = 1/(1 - 2D)$ to $B = D + 1/(-D^2 - 2D + 1)$. Similarly, the output peak phase voltage V_{ac} is increased by a factor of B. The boost factor versus the shoot-through duty ratio and the voltage gain versus the modulation index is plotted for the traditional qZSI and the proposed qZSI with SL circuit configuration in Figure 6 and Figure 7 respectively.

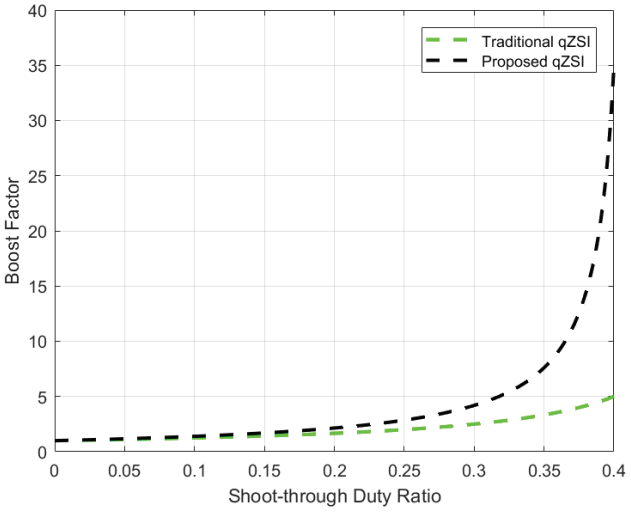

Figure 6. Boost factor versus shoot-through duty ratio.

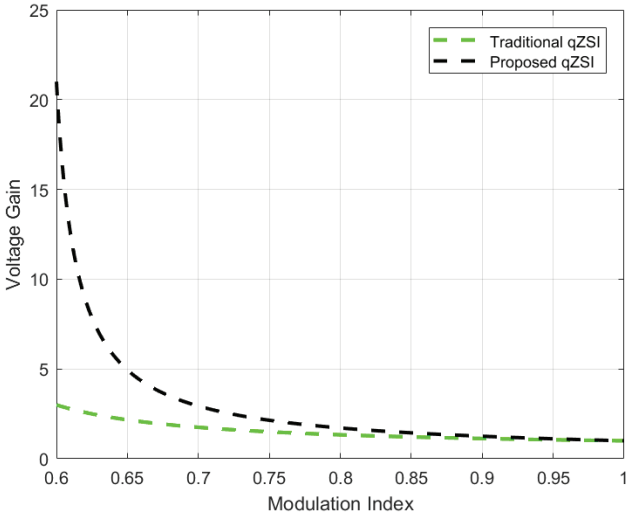

Figure 7. Voltage gain versus modulation index.

Based on the PWM methods; for ZSI/qZSI topologies there are simple boost, maximum boost, and maximum constant boost modulation techniques to control the power switches. All of the three boost control techniques have higher voltage gain compared to traditional PWM [6]. In the proposed qZSI with SL circuit configuration, the simple boost control strategy has been employed for the power switches. This modulation technique has equally spread shoot-through states and as a result, the inductor current and capacitor voltage of the impedance network have no low-frequency ripples. The block scheme and waveforms of the simple boost control technique are shown in Figure 8. In this modulation technique, two straight envelope lines, reference signals, and high-frequency carrier signal are employed to control the shoot-through operation. When the carrier signal is greater than the upper straight envelope line V_p, or lower than the bottom straight envelope line V_n the qZSI circuit is turned into a shoot-through state with a constant shoot-through duty ratio. Otherwise, the circuit switches in the same way as the traditional carrier-based PWM inverter [1].

For the simple boost control technique, the relation between the modulation index and the shoot-through duty ratio can be written as in Eq. (11). As it can be noted from Eq. (10), D will decrease with the increase of M.

$$V_{ac} = MV_{PN} = MBV_{DC} = M\frac{D+1}{-D^2-2D+1}V_{DC} \quad (10)$$

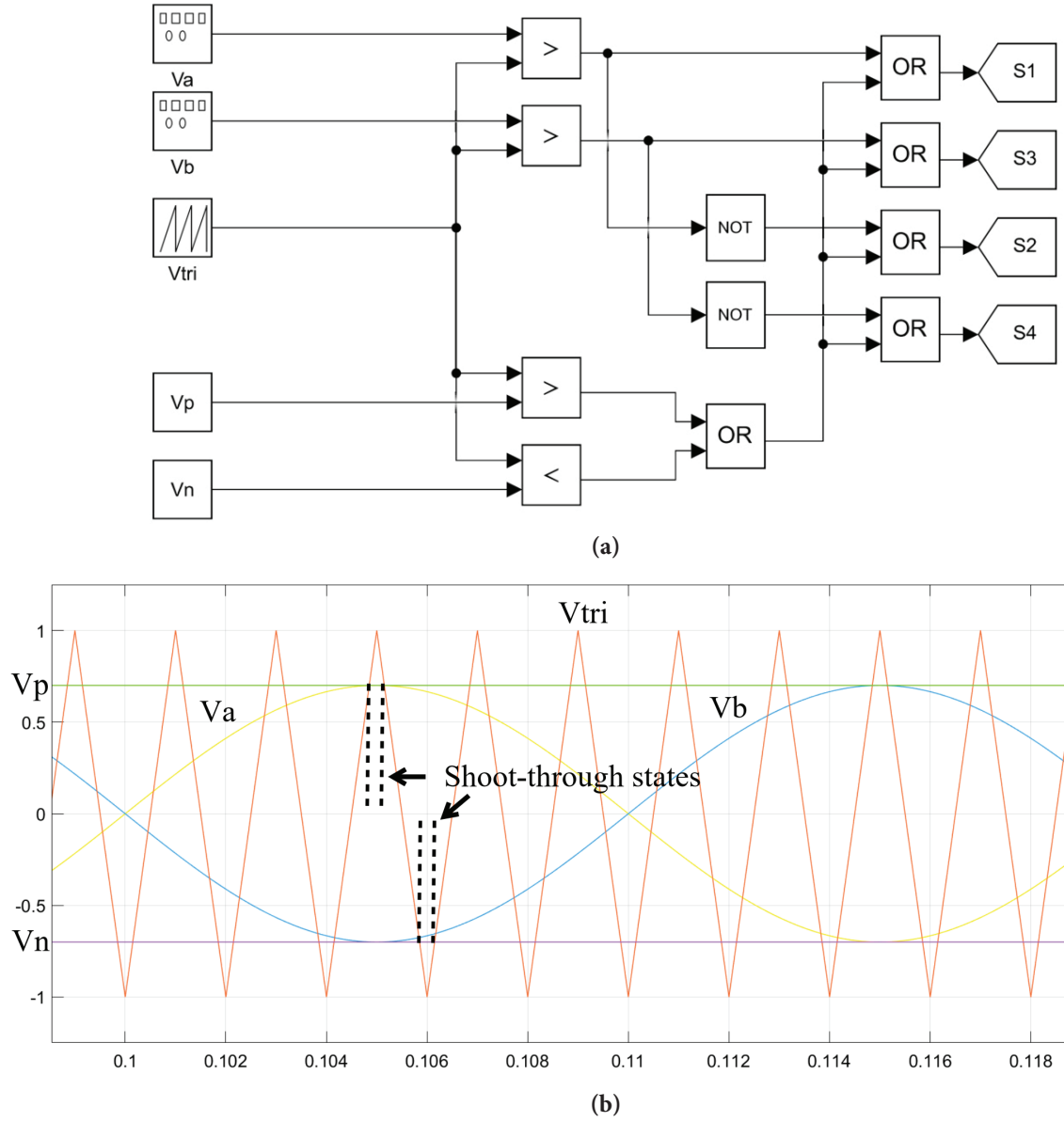

Figure 8. a) Simple boost control block scheme. **b)** Simple boost control waveforms.

RESULTS AND DISCUSSION

The simulation of the proposed single-phase qZSI with SL circuit configuration has been carried out using Matlab/Simulink environment which is widely applied in academic studies and engineering applications and provides scientists design flexibility and operational reliability. To prove the theoretical results, a simulation and experimental setup have been conducted to obtain the required AC output voltage. Therefore the parameters of the proposed qZSI are selected accordingly. The DC voltage V_{DC} = 100V, the switching frequency f_S = 2.5kHz, the load R_L = 10Ω. The inductors of the SL circuit and qZSI network $L_1 = L_2 = L_3$ = 1000μH, and the capacitors of the qZSI network $C_1 = C_2$ = 1000μF, the filter inductance L_f = 500μH and the filter capacitor C_f = 20μF. For the voltage conversion from the DC input 100V, the modulation index should be 0.7 according to the theoretical analysis of the proposed qZSI. Using Eq. (10), when the modulation index is selected as 0.7, the shoot-through duty ratio is determined as 0.3. Under the simple boost control technique with M= 0.7, the corresponding values are obtained using the Eqs. (7), (8) and (9): B = 4.2, G = 2.95, V_{C1} = 295V, V_{C2} = 125V and V_{PN} = 420V. The peak voltage of the fundamental frequency V_{ac} is found to be about 295V. The circuit diagram and the hardware setup of the proposed qZSI are presented in Figure 9.

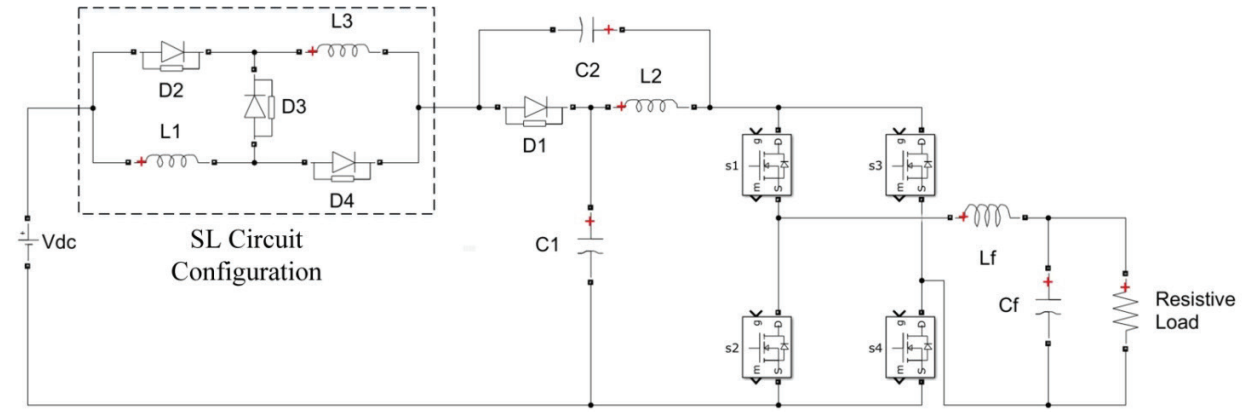

(a)

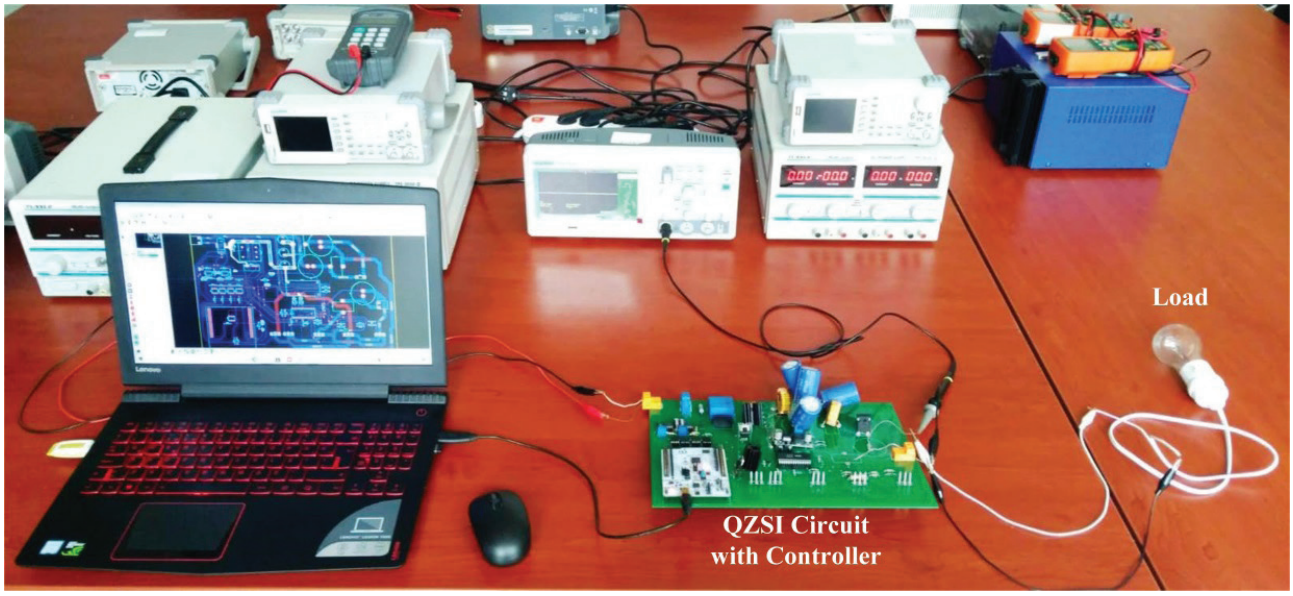

(b)

Figure 9. a) The circuit diagram of the proposed qZSI. **b)** The hardware setup of the proposed qZSI.

The switch voltage and current waveforms are depicted in Figure 10. The simulations and experimental results of the laboratory prototype are given in Figure 11, Figure 12, and Figure 13 respectively. The implementation of the modulation technique for the hardware setup has been realized using a high-performance STM32 Nucleo development board.

As it can be noticed, the steady-state performance from the simulation results is equal to the performed theoretical analysis. Since the shoot-through duty ratio in the simple boost control technique is constant as shown in Figure 8, the oscillation in the passive components is prevented which is important for the power quality. Figure 10 indicates the gate pulses of the switches S_1 and S_2 on the same phase leg. As seen in Figure 10, the charge-discharge behavior of the capacitor during the switching process is linear which helps to reduce the ripples and the harmonic content of the proposed qZSI.

As shown in the simulation and experimental results, the capacitor voltages V_{C1} and V_{C2} of the qZSI network and DC-link voltage V_{PN} across the inverter bridge are boosted to 295V, 125V, and 420V respectively. On the AC side, the peak voltage of the fundamental frequency V_{ac} is obtained around 295V. For the case of the traditional qZSI circuit

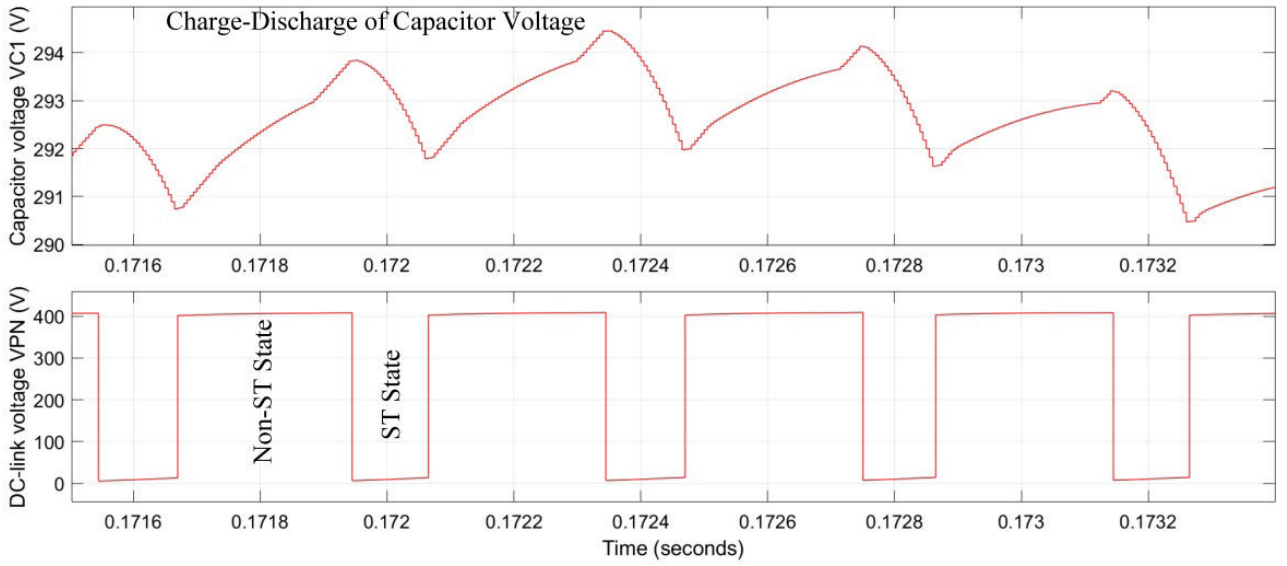

(a)

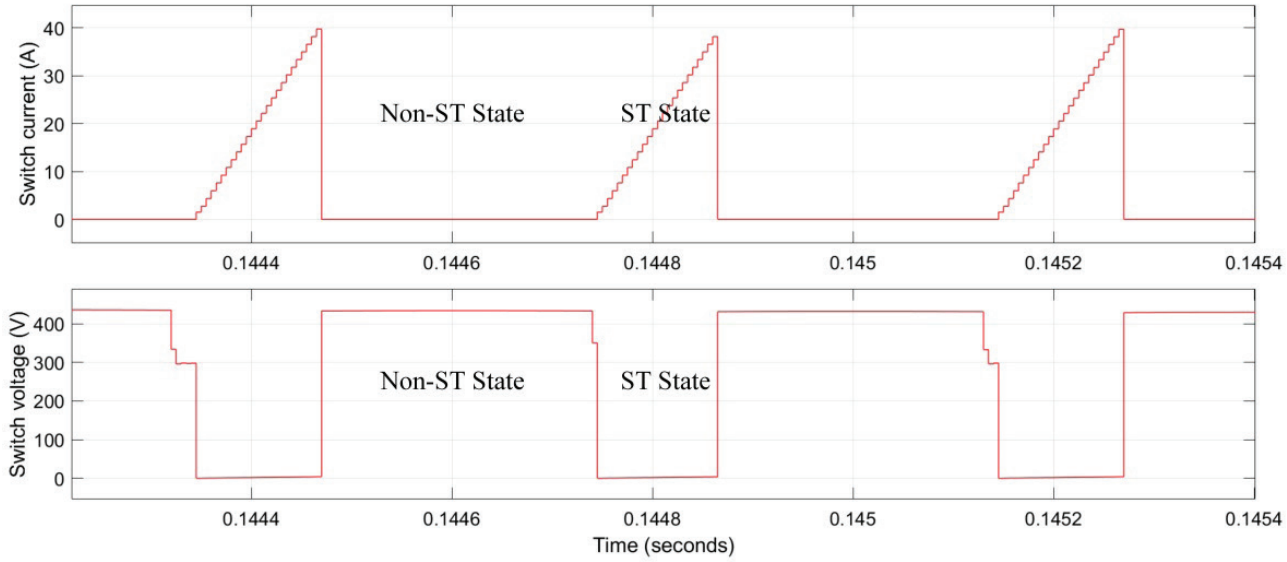

(b)

Figure 10. a) Charge-discharge of capacitor voltage. **b)** Switch voltage and current waveforms.

under the simple boost control technique with the same parameters, the corresponding values would be as follows: B = 2.5, G = 1.75, V_{C1} = 175V, V_{C2} = 75V and V_{PN} = 250V. The peak voltage of the fundamental frequency V_{ac} would increase to 175V. It can be concluded that the boost factor and the voltage conversion ability of the traditional qZSI are much lower than the proposed qZSI. Accordingly, to get the same results a higher shoot-through duty ratio should be used which affects the power quality adversely. In other words, the proposed qZSI employs a higher modulation index for a determined voltage gain and therefore it would need a lower DC input voltage and switching stress compared to the traditional qZSI. Under the same conditions, B, V_{C1}-V_{C2}, V_{PN}, and V_{ac} for simulation and experimental results are listed in Table 1 for the traditional qZSI and the proposed qZSI.

Table 1. Results of the circuit parameters

Circuit Parameter (V_{DC}=100V and M=0.7)	**B**	**V_{C1}-V_{C2}**	**V_{PN}**	**V_{ac}**
Traditional qZSI	2.5	175V-75V	250V	175V
The proposed qZSI	4.2	295V-125V	420V	295V

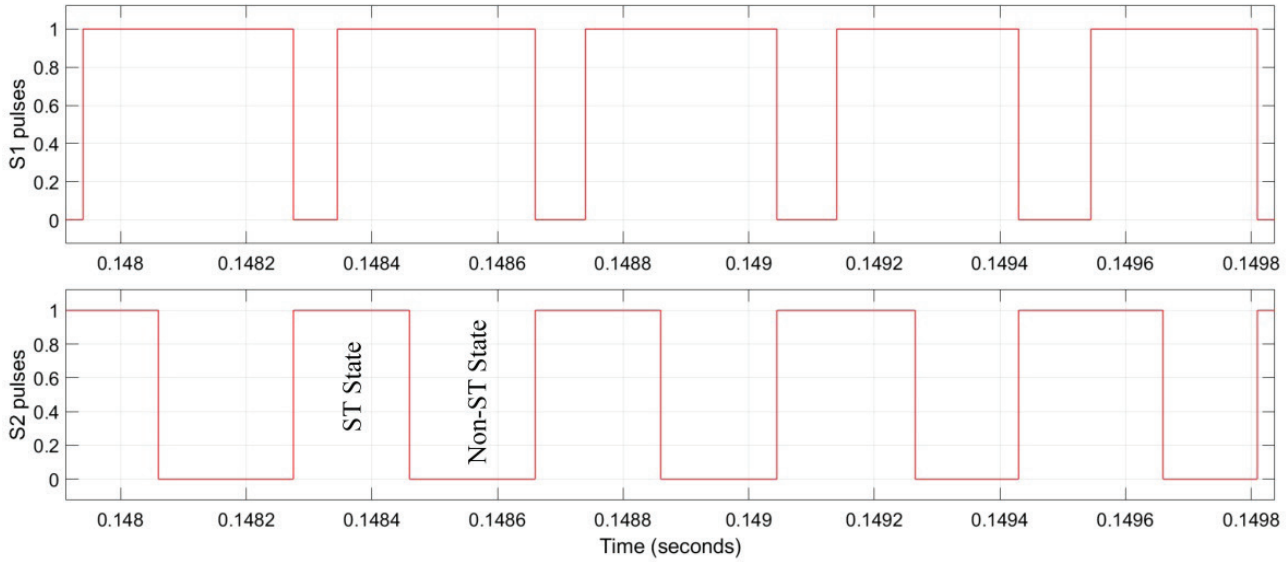

(a)

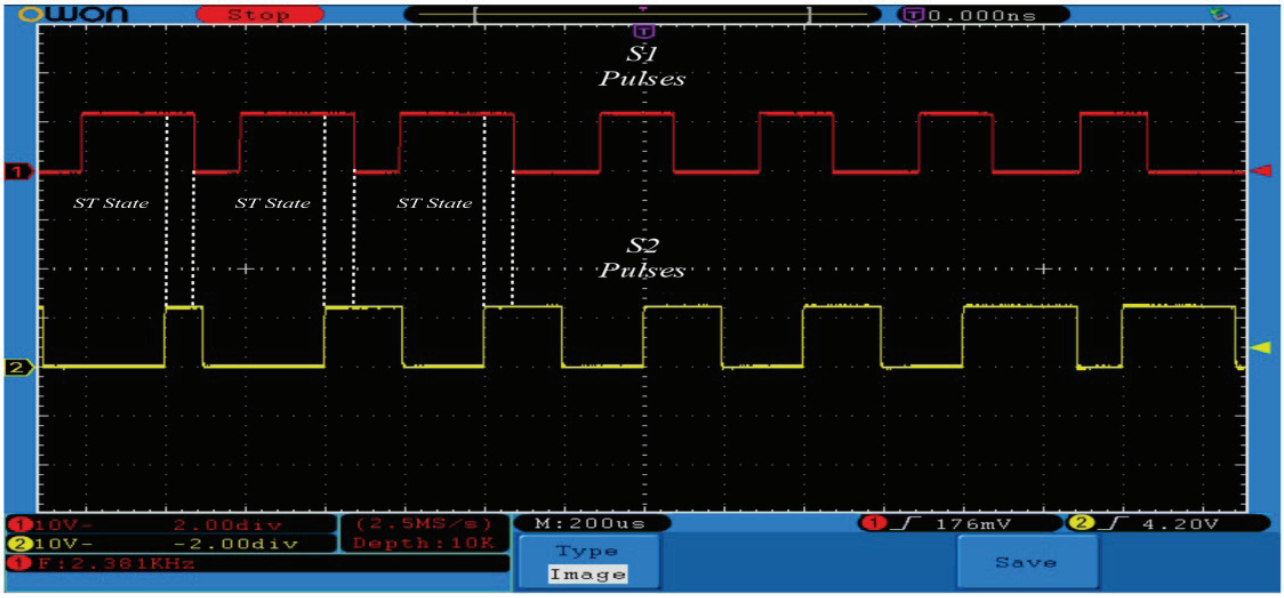

(b)

Figure 11. S_1 and S_2 pulses during operation **a)** Simulation results. **b)** Experimental results.

CONCLUSION

In this study, an improved single-phase qZSI circuit has been presented with SL configuration. Due to the use of the stored DC power in the SL form, the boost factor and the voltage gain of the proposed qZSI are increased. Compared to the traditional ZSI/qZSI circuits, the peak voltage of the fundamental frequency V_{ac} of the proposed qZSI is boosted by 68% at a 0.3 shoot-through duty ratio. For the same voltage conversion ratio, the proposed qZSI would use a higher modulation index and a lower DC voltage source.

The operation principle of the proposed circuit is analyzed with mathematical calculations and simulations. To substantiate the simulation results, a hardware circuit has been tested to get $300V_{pp}$ at the AC side under the simple boost control technique. According to the simulation and experimental results, the proposed qZSI provides a higher voltage conversion ability compared to the traditional qZSI topology. The main drawback of the proposed qZSI will be a small increase in the system cost due to the use of some additional passive circuit elements in the qZSI network which can be ignored considering the overall circuit advantages. For further studies, the proposed circuit conducted

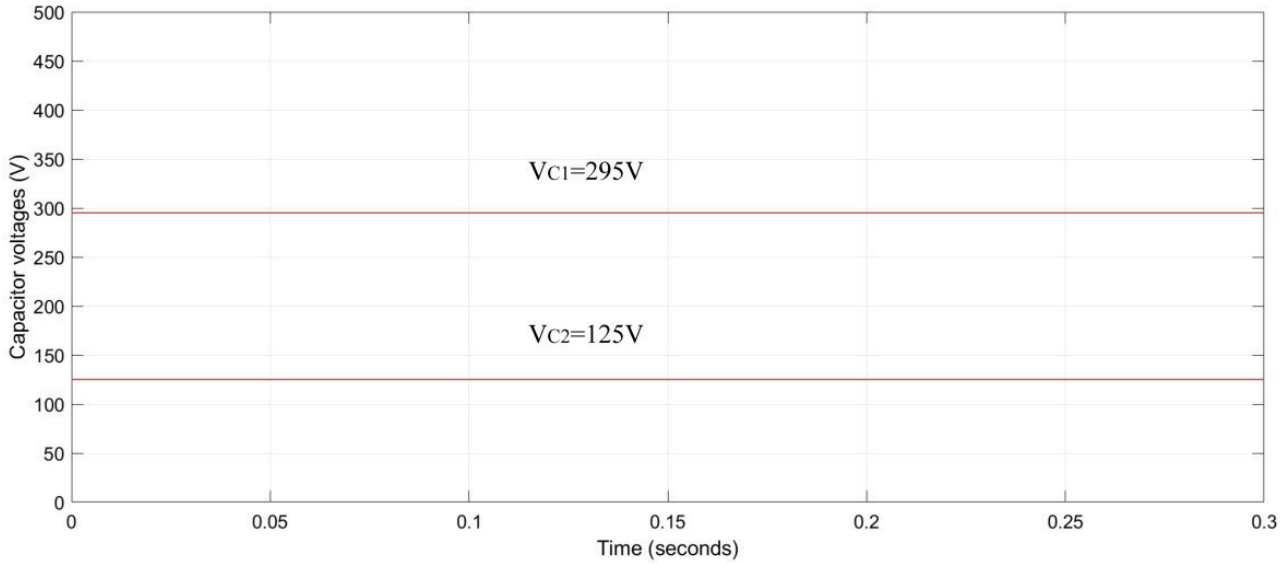

(a)

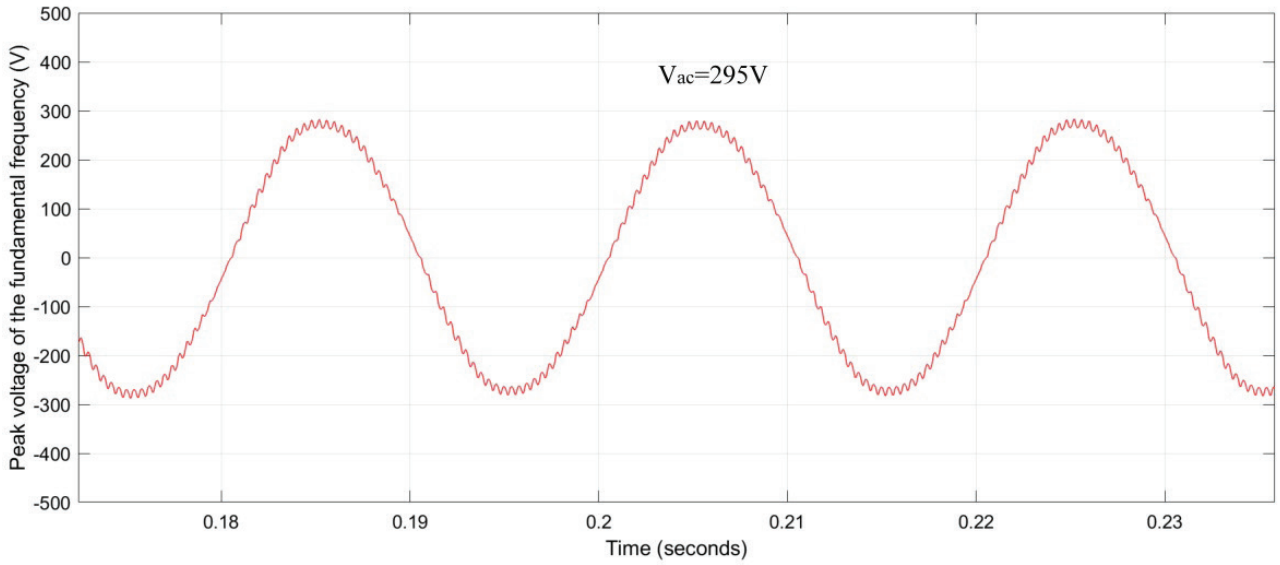

(b)

Figure 12. Simulation results **a)** V_{C1}-V_{C2} voltages. **b)** V_{ac} voltage.

in this paper can be developed by different control strategies and circuit configurations to eliminate the conceptual and theoretical limitations.

AUTHOR CONTRIBUTION

MSE completed this study and wrote the paper. RA read and approved the final paper.

FUNDING INFORMATION

There are no funders to report for this submission.

DATA AVAILABILITY STATEMENT

No new data were created in this study. The published publication includes all graphics collected or developed during the study.

CONFLICT OF INTEREST

The author declared no potential conflicts of interest with respect to the research, authorship, and/or publication of this article.

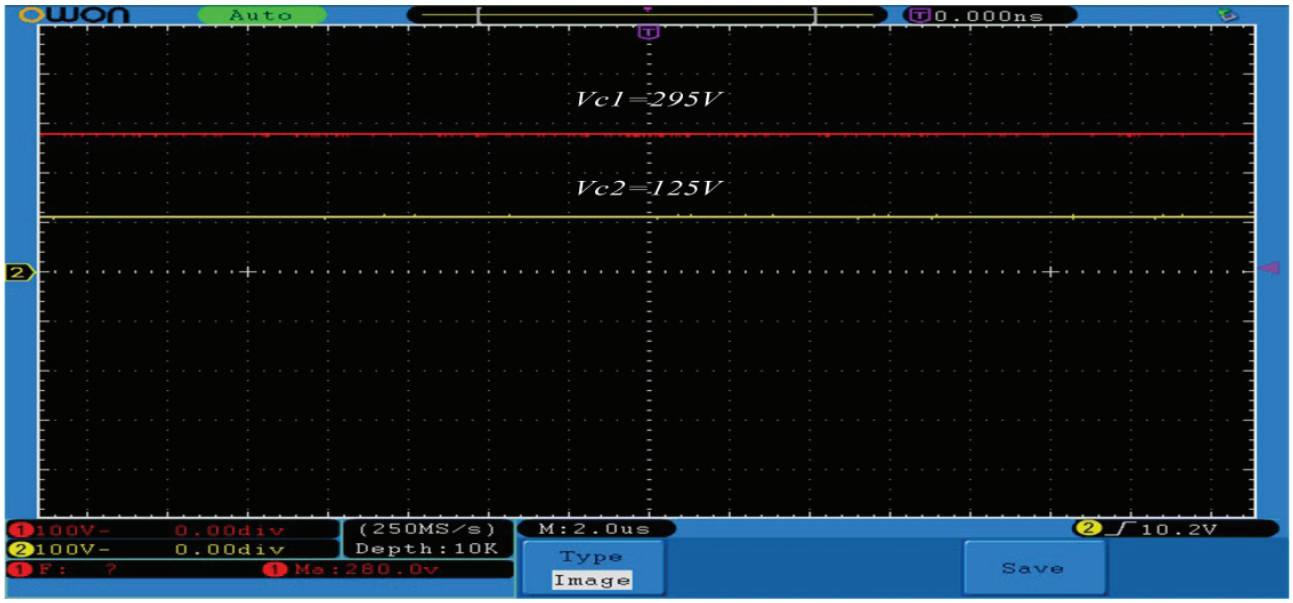

(a)

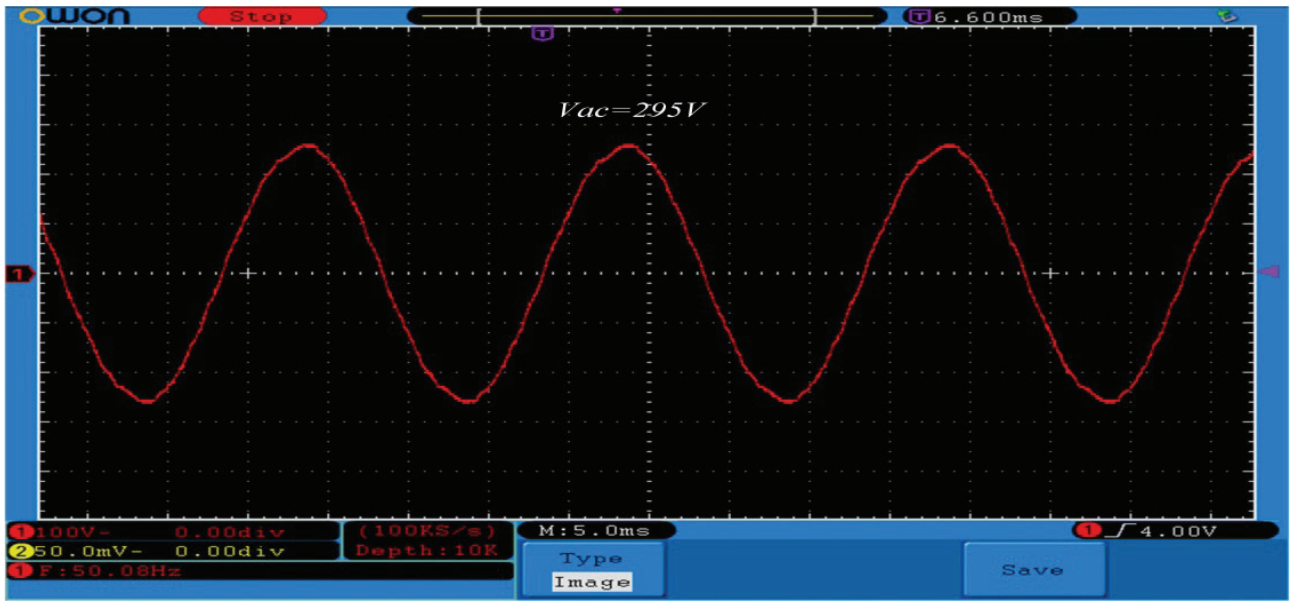

(b)

Figure 13. Experimental results **a)** V_{C1} and V_{C2} voltages. **b)** V_{ac} voltage.

REFERENCES

[1] Peng FZ. Z-source inverter. IEEE Trans Ind Appl 2003;39:504–510. [CrossRef]

[2] Mande D, Trovão JP, Ta MC. Comprehensive review on main topologies of impedance source inverter used in electric vehicle applications. World Electr Veh J 2020;11:37. [CrossRef]

[3] Subhani N, Kannan R, Mahmud A, Blaabjerg F. Z-source inverter topologies with switched Z-impedance networks: A review. IET Power Electr 2021;14:727–750. [CrossRef]

[4] Anderson J, Peng FZ. Four quasi-Z-source inverters. 2008 IEEE Power Electronics Specialists Conference; 2008 Jun 15-19; Rhodes, Greece: IEEE; 2008. pp. 2743–2749. [CrossRef]

[5] Noroozi N, Zolghadri MR. Three-phase quasi-Z-source inverter with constant common-mode voltage for photovoltaic application. IEEE Trans Ind Electron 2017;65:4790–4798. [CrossRef]

[6] Ellabban O, Abu-Rub H. Z-source inverter: Topology improvements review. IEEE Ind Electron Mag 2016;10:6–124. [CrossRef]

[7] Siwakoti YP, Peng FZ, Blaabjerg F, Loh PC, Town GE. Impedance-source networks for electric power conversion part I: A topological review. IEEE Trans Power Electron 2014;30:699–716. [CrossRef]

[8] Siwakoti YP, Peng FZ, Blaabjerg F, Loh PC, Town GE, Yang S. Impedance-source networks for electric power conversion part II: Review of control and modulation techniques. IEEE Trans Power Electron 2014;30:1887–1906. [CrossRef]

[9] Nguyen MK, Lim YC, Cho GB. Switched-inductor quasi-Z-source inverter. IEEE Trans Power Electron 2011;26:3183–3191. [CrossRef]

[10] Nguyen MK, Lim YC, Choi JH. Two switched-inductor quasi-Z-source inverters. IET Power Electron 2012;5:1017–1025. [CrossRef]

[11] Lashab A, Sera D, Martins J, Guerrero JM. Dual-input quasi-z-source PV inverter: Dynamic modeling, design, and control. IEEE Trans Ind Electron 2019;67:6483–6493. [CrossRef]

[12] Jagan V, Kotturu J, Das S. Enhanced-boost quasi-Z-source inverters with two-switched impedance networks. IEEE Trans Ind Electron 2017;64:6885–6897. [CrossRef]

[13] Ahmad A, Singh R. Topologies of switched-inductor switched-capacitor based enhanced boost z-source inverters for renewable energy applications. 2018 IEEE Energy Conversion Congress and Exposition; 2018 Sep 23-27; Portland, USA: IEEE; 2018. pp. 6674–6681. [CrossRef]

[14] Pan L. LZ-source inverter. IEEE Trans Power Electron 2014;29:6534–6543. [CrossRef]

[15] Abbasi M, Eslahchi AH, Mardaneh M. Two symmetric extended-boost embedded switched-inductor quasi-Z-source inverter with reduced ripple continuous input current. IEEE Trans Ind Electron 2017;65:5096–5104. [CrossRef]

[16] Yuan J, Yang Y, Blaabjerg F. A switched quasi-Z-Source inverter with continuous input currents. Energies 2020;13:1390. [CrossRef]

[17] Karaarslan A, Al-Darraji O, Calıkoglu D. Two new impedance source network topologies for inverter applications. Int J Electron 2019;106:599–619. [CrossRef]

[18] Abid A, Zellouma L, Bouzidi M, Lashab A, Rabhi B. Switched inductor z-source/quasi z-source network: State of art and challenges. 2020 1st International Conference on Communications, Control Systems and Signal Processing; 2020 May 16-17; El Oued, Algeria: IEEE; 2020. pp. 477–482. [CrossRef]